EBERHARD KARLS
UNIVERSITÄT
TÜBINGEN

Mathematisch-Naturwissenschaftliche Fakultät
Institut für Astronomie und Astrophysik
Kepler Center for Astro and Particle Physics

XMM-Newton observations of the supernova remnants [HP99] 1139 and 1RXS J053353.6-720404 in the Large Magellanic Cloud

E.T. Whelan[1], P.J. Kavanagh[1], M.Sasaki[1], P. Maggi[2], F. Haberl[2], L.M. Bozzetto[3], M.D. Filipović[3], E. Crawford[3]

1) Institut für Astronomie und Astrophysik, Eberhard Karls Universität Tübingen, Sand 1, 72076 Tübingen, Germany
2) Max-Planck-Institut für extraterrestrische Physik, Giessenbachstraße, D-85748 Garching, Germany
3) University of Western Sydney, Locked Bag 1797, Penrith South DC, NSW 1797, Australia

Supernova remnants (SNRs) are of vital importance to the physical and chemical evolution of the interstellar medium (ISM). The expanding shell of the remnants imparts kinetic energy to the surrounding ISM as well as enriching it with the metals fused in the cores of their progenitor stars. Thus, an understanding of these objects is crucial to the understanding of star formation and matter recycling in galaxies. The evolution of SNRs can best be studied in soft X-ray line and continuum emission, since they mainly consist of very hot plasma (10^6-10^7 K). We have been studying SNRs in the Large Magellanic Cloud (LMC) in greater detail using combined optical, radio, and X-ray observations. The X-ray selected candidate SNRs 1RXS J053353.6–720404 and [HP99] 1139 were observed by *XMM-Newton* in May 2013. Both objects are readily apparent as SNRs due to their soft thermal X-ray emission and morphology. [HP99] 1139 is notable due to the bright Fe-rich gas in its interior, a feature observed in several evolved LMC SNRs and is typical of a Type Ia SN progenitor. In this poster we present the X-ray analysis of these two remnants.

X-ray Observations, Imaging and Spectral Analysis

XMM-Newton observations of [HP99] 1139 (~30 ks) and 1RXS J053353.6−720404 (~30 ks) were carried out on May 3 and 9 2013 (Obs. IDs 0720440201 and 0651880201, PI M. Sasaki), respectively. The primary instrument for the observations was the European Photon imaging Camera (EPIC) onboard *XMM-Newton* (Jansen et al. 2001). The data were reduced using the standard reduction tasks of SAS Version 13.5.0, filtering for periods of high particle background. Detector background-subtracted, vignetting corrected, and adaptively smoothed Images were produced in various energy bands from the flare filtered event lists. We used three energy bands suited to the analysis SNR spectra, namely 0.3 to 0.7 keV (strong lines from oxygen); 0.7 to 1.1 keV (Fe L-shell lines, Ne Heα and Lyα lines); and 1.1 to 4.2 keV (lines from Mg, Si, S, Ca, Ar, and possibly non-thermal continuum). Point source detection was performed using the SAS meta-task *edetect_chain* across all the EPIC detectors in several energy bands. False detections due to the bright diffuse emission of the target SNRs were removed from the source list. The remaining sources were masked for our analysis. Using the images, we defined spectral extraction regions for the remnants. To constrain the astrophysical background we extracted spectra from nearby regions and fitted these simultaneously with the SNR spectra, using standard X-ray background model components with appropriate fit parameters linked. We additionally extracted spectra from filter-wheel-closed data to account for the detector background in the fits. We also note here that in the spectral analysis of each remnant, an additional model component was required to account for residual soft-proton contamination. All spectra were re-binned so that each bin contained a minimum of 30 counts, enabling the use of the χ^2 statistic. All fits were performed using XSPEC version 12.8.1 with abundance tables set to those of Wilms et al. (2000), and photoelectric absorption cross-sections set to those of Balucinska-Church & McCammon (1992). A more detailed description of the imaging and spectral methods used can be found in, e.g., Bozzetto et al. (2014) and Maggi et al. (2014).

[HP99] 1139

The X-ray morphology of [HP99] 1139 is notable due to the central bright emission in the 0.7-1.1 keV band (see Fig. 1). This is consistent with an evolved Fe-rich remnant and adds to the growing number of these objects. Other LMC examples are DEM L238 and DEM L249 (Borkowski et al., 2006), MCSNR J0508-6902 (Bozzetto et al., 2014), and MCSNR J0508−6830 and MCSNR J0511−6759 (Maggi et al., 2014). The dimensions of [HP99] 1139 were found to be ~80 x 52 pc, making it one of the larger remnants in the LMC.

We extracted EPIC spectra from the shell and interior regions of [HP99] 1139. Given the size of the remnant, we assumed that the remnant is into the Sedov phase of its evolution. We fitted the shell spectra with various thermal plasma models appropriate for SNRs in this stage, and report here on the results of the plane parallel shock model (*vpshock* in *XSPEC*). The results are given in Table 1, with the data and best-fit model in Fig. 2. We determined a shell temperature of kT = 0.54 (0.51-0.57) keV and an upper limit to the ionisation timescale distribution of τ_u = 5.92 (4.96-7.45) x 10^{11} s cm^{-3}, indicating that the plasma is close to collisional ionisation equilibrium (CIE).

Fits to the interior spectrum of [HP99] 1139 included a component accounting for the the contamination due to the shell. Trial fits demonstrated an obvious over abundance of Fe in the interior, as expected from the imaging analysis, and that the Fe-rich component was in CIE. Following the method used in Kosenko et al. (2010), Bozzetto et al. (2014), and Maggi et al. (2014), we applied a more physical multi-component model, with each component representing a pure metal plasma in the interior. It was found that, apart from the Fe component, a minimal, but significant, pure O component was required. The fit results are given in Table 1 with the best-fit spectrum in Fig. 2. The temperature of the O component was found to be different than that of the Fe, and it is unclear whether these plasmas are co-spatial. We estimated the mass of Fe in the interior assuming that O component is not co-spatial and supplies no electrons to the Fe-rich gas. We determined the mass of Fe in the interior assuming the limiting cases of admixture of H in the Fe ejecta as discussed in Hughes et al. (2003), and for non-clumpy and clumpy ejecta (Kosenko et al. 2010). We found that the case of a clumpy ejecta, with comparable amount of H mixed in to the Fe-rich gas, provided an Fe mass of 0.9-1 $M_\odot$, which is close to the expected yield of a Type Ia (Iwamoto et al., 1999). We estimated the physical properties of [HP99] 1139 using the combined fit results of the shell emission (interior plus shell fits) and the Sedov dynamical model. A detailed description of this method can be found in e.g., Bozzetto et al. (2014) and Maggi et al. (2014). We determined an age of 17-21 kyr for the remnant, an initial explosion energy of (0.4-1.8) x 10^{51} erg, and a swept-up mass of 90-191 $M_\odot$.

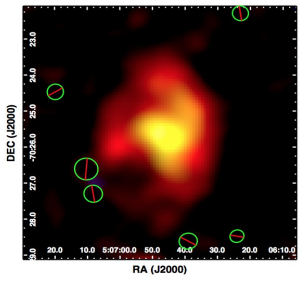

Figure 1: XMM-Newton EPIC image of [HP99] 1139 in false colour with RGB corresponding to 0.3–0.7 keV, 0.7–1.1 keV, and 1.1–4.2 keV. Regions excluded due to point sources are indicated.

Table 1: Spectral fit results for [HP99] 1139

Component	Parameter	Value
	Shell: vpshock	
phabs	$N_{H,Gal}$ (10^{22} cm^{-2})	0.07[a]
vphabs	$N_{H,LMC}$ (10^{22} cm^{-2})	< 0.01[b]
vpshock[c]	kT	0.54 (0.51–0.57)[d]
	τ_u (10^{11} s cm^{-3})	5.92 (4.96–7.45)
	EM (10^{57} cm^{-3})	6.40 (5.95–6.91)
	L_X[e] (10^{35} erg s^{-1})	1.5
Fit statistic	χ^2_ν	1.25 (214 d.o.f)
	Interior: vpshock + vpshock + vpshock	
vpshock (Fe)	kT	0.64 (0.63–0.66)
	$norm$ (10^{-4} cm^{-5})	1.95 (1.77–2.09)
vpshock (O)	kT	0.10 (< 0.16)
	$norm$ (10^{-4} cm^{-5})	6.15 (0.35–8.99)
	L_X[e] (10^{35} erg s^{-1})	0.6
Fit statistic	χ^2_ν	1.12 (172 d.o.f.)

Notes. [a] Fixed to the Galactic column density from the Dickey & Lockman (1990) HI maps. [b] Absorption component abundances fixed to those of the LMC. [c] Abundances fixed to those of the LMC. [d] The numbers in parentheses are the 90% confidence intervals. [e] 0.3-10 keV de-absorbed X-ray luminosity, adopting a distance of 50 kpc to the LMC.

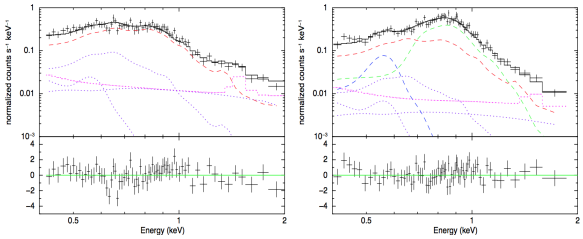

Figure 2: Best-fit models to the shell (left) and interior (right) of [HP99] 1139. In each panel, the purple dotted lines indicate the astrophysical background components, the magenta dotted lines represent the combined detector and particle background components, and the red dashed line marks the shell emission components. In the right panel, the green dashed line indicates the pure Fe component with the blue dashed line marking the pure O component. In each case, only the EPIC-pn remnant spectrum is shown for clarity.

1RXS J053353.6-720404

The X-ray morphology of 1RXS J053353.6 720404 was found to be consistent with the horse-shoe radio morphology determined in Bozzetto et al. (2013), who refer to the remnant as SNR J0533-7202. From the X-ray data, we found the dimensions of the SNR to be ~57 x 47 pc (Fig. 3)

We followed the same spectral analysis procedure as for the shell of [HP99] 1139, and fitted the remnant spectra with various thermal plasma models, and report on the results of the *vpshock* model. The fit results are given in Table 2, with the data and best-fit model shown in Fig. 4. As above, we estimated the physical properties of 1RXS J053353.6−720404 from the Sedov dynamical model. We determined an age of 14-21 kyr for the remnant, an initial explosion energy of (0.2-1.1) x 10^{51} erg, and a swept-up mass of 47-121 $M_\odot$.

Bozzetto et al. (2013) assessed the local stellar population and star formation history of the region around 1RXS J053353.6−720404, and found that the remnant is associated with an old stellar population. This points to a Type Ia origin. We detected a point source close to the centre of the SNR, which was found not to have a multi-wavelength counterpart. The source was too faint for a rigorous spectral analysis, but its X-ray colours suggest that it is much more absorbed than is expected for an LMC source. Thus we conclude that this source is most likely a background AGN and not associated with 1RXS J053353.6−720404.

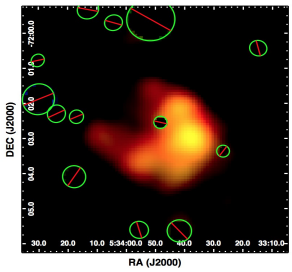

Figure 3: XMM-Newton EPIC image of 1RXS J053353.6-720404 in false colour with RGB corresponding to 0.3–0.7 keV, 0.7–1.1 keV, and 1.1–4.2 keV. Regions excluded due to point sources are indicated. We note that the X-ray colours of the point source located at the centre of the remnant indicate that it is most likely a background AGN.

Table 2: Spectral fit results for 1RXS J053353.6-720404

Component	Parameter	Value
	vpshock	
phabs	$N_{H,Gal}$ (10^{22} cm^{-2})	0.07[a]
vphabs	$N_{H,LMC}$ (10^{22} cm^{-2})	0.08 (0.01–0.17)[b,c]
vpshock	kT	0.44 (0.32–0.66)[b]
	τ_u (10^{10} s cm^{-3})	4.67 (2.40–9.14)
	EM (10^{57} cm^{-3})	3.74 (2.00–7.54)
	F_X[c] (10^{-13} erg s^{-1} cm^{-2})	4.7
	L_X[d] (10^{35} erg s^{-1})	1.4
Fit statistic	χ^2_ν	1.20 (257 d.o.f.)

Notes. [a] Fixed to the Galactic column density from the Dickey & Lockman (1990) HI maps. [b] Absorption and thermal component abundances fixed to those of the LMC. [c] 0.3-10 keV de-absorbed X-ray flux. [d] 0.3-10 keV de-absorbed X-ray luminosity, adopting a distance of 50 kpc to the LMC. [e] The numbers in parentheses are the 90% confidence intervals.

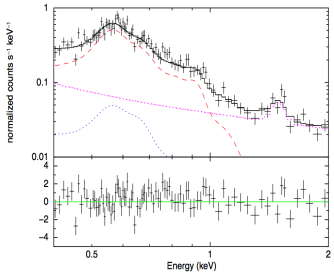

Figure 4: Best-fit model to the spectrum of 1RXS J053353.6−720404. The purple dotted lines indicate the astrophysical background components, the magenta dotted lines represent the combined detector and particle background components,and the red dashed line marks the SNR emission component. Only the EPIC-pn remnant spectrum is shown for clarity.

References

Balucinska-Church & McCammon 1992, ApJ, 400, 699
Borokowski et al. 2006, ApJ, 652,1259
Bozetto et al. 2013, MNRAS, 432, 2177
Bozetto et al. 2014, MNRAS, 439, 1110
Dickey & Lockman 1990, ARA&A, 28, 215
Iwamoto et al., 1999, ApJ, Suppl., 125, 439
Jansen et al. 2001, A&A, 365, L1
Kosenko et al. 2010, A&A, 519, A11
Maggi et al. 2014, A&A, 561, A76
Wilms et al. 2000, ApJ, 542, 914

This work is funded through the Bundesministerium für Wirtschaft und Technologie/Deutsches Zentrum für Luft- und Raumfahrt (BMWi/DLR) grant FKZ 50 OR 1309.
E. W. acknowledges f nancial support from the Deutsche Forschungsgemeinschaft (DFG) through the Research Grant Wh 172/1-1. M. S. acknowledges support from the Emmy Noether Research Grant SA 2131/1-1 of the DFG . P. M. acknowledges support form BMWi/DLR grant FKZ 50 OR 1201.

Contact: whelan@astro.uni-tuebingen.de

Emmy Noether-Programm Deutsche Forschungsgemeinschaft DFG

DFG Deutsche Forschungsgemeinschaft

DLR